

Composite Laminate Free-Edge Reinforcement with U-Shaped Caps

Part II: Theoretical-Experimental Correlation

W. E. Howard,* Terry Gossard Jr.,† and Robert M. Jones‡

Virginia Polytechnic Institute and State University, Blacksburg, Virginia

Generalized plane strain finite-element analysis is used to predict significant reduction of interlaminar normal stresses when a U-shaped cap is bonded to the edge of a composite laminate in Part I. Three-dimensional composite material failure criteria are used in a progressive laminate failure analysis to predict failure loads of laminates with different edge-cap designs. Experimentally, symmetric 11-layer graphite-epoxy laminates with a one-layer cap of Kevlar-epoxy cloth are shown to carry 130–140% more load than uncapped laminates under static tensile and tension-tension fatigue loading. In addition, the coefficient of variation of the static tensile failure load decreases from 24% to 8% when edge caps are added. The predicted failure load calculated with the finite-element results is 10% lower than the actual failure load. For both capped and uncapped laminates, actual failure loads are much lower than those predicted using classical lamination theory stresses and a two-dimensional failure criterion. Possible applications of the free-edge reinforcement concept are described, and future research is suggested.

1. Introduction

HOWARD, Gossard, and Jones¹ show that interlaminar normal stresses in the composite laminate free-edge delamination problem are reduced significantly by the use of edge-cap reinforcement. Moreover, O'Brien² has observed that mode I (normal-stress-dominated) failure determines free-edge delamination. Accordingly, the fundamental working hypothesis is that edge caps are effective because they suppress the primary delamination mechanism. The efforts of Howard, Gossard, and Jones in Part I of this two-part paper are addressed to the stress analysis behind the multi-event failure process that begins with initial delamination and proceeds through degradation of some lamina properties to ultimate laminate failure. That progressive failure process is examined in this paper.

The laminate studied is the 11-layer NASA edge delamination specimen with stacking sequence $[+30/-30/+30/-30/90/90/90/-30/+30/-30/+30]$.³ The method of reinforcement is a simple U-shaped edge cap made by wrapping a single layer of Kevlar-49 style-120 cloth impregnated with F-155 epoxy resin around the T-300-5209 graphite-epoxy laminate edge as shown in Fig. 1.

Failure predictions are addressed in Sec. II with attention being focused on two- as well as three-dimensional stress states. Progressive failure is modeled with three-dimensional stresses from the first part of this paper. Progressive failure modeling was attempted with a midplane node release approach. However, use of that approach merely resulted in moving the highly stressed region away from the edge to the last unreleased node. Accordingly, the various moduli are degraded as described in Sec. II. The contrast between the two approaches is that the node release concept has the penalty of elimination of *all* connectivity between regions, whereas the degradation approach

has the benefit of retaining *some* connectivity if the nature of the failure is consistent with that model. Next, laminates are fabricated with edge caps and subjected to static tensile loading to failure as well as to constant-amplitude tension-tension fatigue loading. Fabrication problems are described as are the various test results that are correlated with theoretical results in Sec. III. Finally, in Sec. IV, conclusions are drawn and significant applications of edge-cap reinforcement are described along with suggestions for future research.

II. Failure Predictions

A progressive laminate failure analysis is used to predict the failure load of the reinforced NASA edge delamination tension specimen.² Common failure criteria are used to predict the failure loads of individual laminae. The material properties of the lamina with the lowest failure load are then degraded to reflect the associated failure mode. The analysis is repeated until no laminae remain intact, i.e., until gross laminate failure occurs.

A. Lamina Failure Criteria

Classical lamination theory and finite-element analysis are used to determine the laminae stresses in the manner of Part I.¹ To relate the stresses to lamina failure, a failure criterion must be used. The three criteria used here—Tsai-Hill,⁴ Hoffmann,⁵ and Tsai-Wu⁶—are among the most widely accepted failure criteria.

For plane stress in the plane of the lamina, five material strengths are required: two uniaxial tensile strengths X_t and Y_t ,

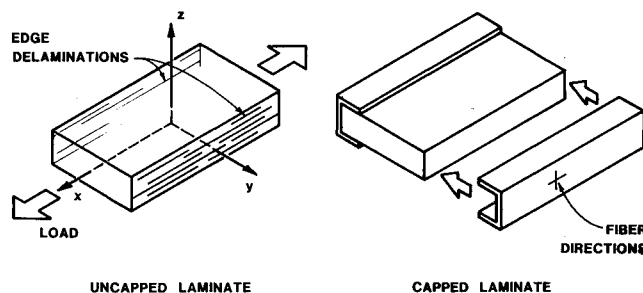


Fig. 1 Free-edge reinforcement.

Received March 25, 1986; revision received Jan. 26, 1988. Copyright © 1988 by Robert M. Jones. Published by the American Institute of Aeronautics and Astronautics, Inc., with permission.

*Formerly Graduate Research Assistant; currently Senior Engineer, Composite Structures Section, Morton-Thiokol Corporation, Brigham City, UT.

†Formerly Undergraduate Student; currently Engineer, Atlantic Research Corporation, Gainesville, VA.

‡Professor of Engineering Science and Mechanics. Associate Fellow AIAA.

two uniaxial compressive strengths X_c and Y_c , and the shear strength S . Those strengths are listed in Table 1 of Ref. 1. The 1-, 2-, and 3-axes are the lamina principal material directions, with the 1-axis coincident with the longitudinal axis of the fibers. The material is regarded as transversely isotropic because the properties in the 3-direction are the same as those in the 2-direction.

The Tsai-Hill⁴ criterion for tensile failure is

$$\frac{\sigma_1^2}{X_t^2} + \frac{\sigma_2^2}{Y_t^2} - \frac{\sigma_1\sigma_2}{X_t^2} + \frac{\tau_{12}^2}{S^2} = 1 \quad (1)$$

The X_t and/or Y_t in Eq. (1) changes to X_c and/or Y_c if the corresponding stresses are compressive. The Hoffman⁵ failure criterion is

$$\frac{\sigma_1^2 - \sigma_1\sigma_2}{X_t X_c} + \frac{\sigma_2^2}{Y_t Y_c} + \frac{(X_c - X_t)\sigma_1}{X_t X_c} + \frac{(Y_c - Y_t)\sigma_2}{Y_t Y_c} + \frac{\tau_{12}^2}{S^2} = 1 \quad (2)$$

The Tsai-Wu⁶ criterion for failure is

$$\frac{\sigma_1^2}{X_t X_c} + \frac{\sigma_2^2}{Y_t Y_c} + \left(\frac{1}{X_t} - \frac{1}{X_c}\right)\sigma_1 + \left(\frac{1}{Y_t} - \frac{1}{Y_c}\right)\sigma_2 + F_{12}\sigma_1\sigma_2 + \frac{\tau_{12}^2}{S^2} = 1 \quad (3)$$

The Tsai-Wu criterion contains one parameter, F_{12} , which must be determined in a biaxial loading test. Usually this test is not practical or desirable, so a value for F_{12} must be chosen based on the tests already performed. Narayanaswami and Adelman⁷ recommend that a value of zero for F_{12} be used to obtain acceptable results, and that approach is adopted herein. If $F_{12} = -1/(X_t X_c)$, then the Hoffman criterion results, and if $F_{12} = -1/X_t^2$ and all tensile and compressive strengths are equal, then the Tsai-Hill criterion results.

All of the foregoing criteria are for failure prediction of a single lamina. For progressive laminate failure, a failure criterion is applied to each lamina individually, and the lamina that fails first is eliminated or has its properties degraded. Then, the loading is increased until another lamina fails, and the process is repeated until all laminae fail. Such a procedure is necessary because failure of a single lamina does not necessarily mean that the entire laminate fails at the corresponding load.

For example, consider a cross-ply laminate (all laminae are oriented with their fibers either parallel to or perpendicular to the laminate x -axis) under uniform tensile load in the x -direction. A failure analysis of each lamina is performed, and matrix failure in the laminae with fibers perpendicular to the x -axis is identified as the first failure mode. The material properties of these laminae are degraded to account for this failure by setting $E_2 = 0$ but retaining E_1 , and a second failure analysis of each lamina is performed. The next failure mode encountered as the load is increased is fiber breakage in the laminae with fibers parallel to the axis. This failure mode is clearly critical for the laminate, i.e., the laminate can no longer support load.

Table 1 Static loading results

	Failure load, lb	Mean failure load, lb	Coefficient of variation, %
Uncapped	2250	1808	24
	1380		
	1500		
	2100		
Capped	3950	4367	8
	4650		
	4500		

B. Failure Predictions Based on Two-Dimensional Stresses

Predicted failure loads calculated using classical lamination theory (CLT) stresses are too high because interlaminar stresses are not accounted for in that theory. These failure loads are of interest, however, because they represent the theoretically highest possible laminate strength, i.e., the strength that would be obtained if the interlaminar stresses did not influence failure.

The failure sequence outlined here results from using the Hoffman criterion. Similar procedures are used to predict the failure load using the Tsai-Hill and Tsai-Wu failure criteria. An axial load per unit width of 1000 lb/in. is arbitrarily selected, and CLT is used to predict the in-plane stresses in principal material directions. The principal material direction stresses in the 90-deg layers are $\sigma_1 = -14,849$ psi, $\sigma_2 = 3,433$ psi, and $\tau_{12} = 0$. The principal material direction stresses in the ± 30 -deg layers are $\sigma_1 = 28,618$ psi, $\sigma_2 = 662$ psi, and $\tau_{12} = \pm 2,406$ psi. Because linear analysis is used, these stresses can be linearly scaled to obtain the state of stress at any load value at or below the first-ply failure load. The stresses for each lamina are scaled to be the load value at which the failure criterion polynomial is equal to one (the condition for lamina failure). Laminate failure loads that result from this scaling are 2617 lb for the 90-deg layers and 5594 lb for the ± 30 -deg layers. Therefore, the 90-deg layers fail first. Each term of the failure criterion polynomial is then evaluated for the 90-deg lamina failure load to determine the failure mode. The largest terms by far are those that involve the stress component transverse to the fibers (in the x -direction) so the matrix (resin) of the 90-deg layers will fail.

To approximately account for this failure in a progressive laminate failure analysis, E_x and G_{xy} for the 90-deg layers are reduced by a factor of 10. Stresses are recalculated, and new laminate failure loads are computed: 5294 lb for the ± 30 -deg layers and 13,875 lb for the 90-deg layers. The individual terms of the failure criterion polynomial are calculated, and the ± 30 -deg layers are predicted to fail in a combined fiber tension and in-plane shear mode. Because this mode results in broken fibers, the laminate will be left with no load-carrying capability. Therefore, 5294 lb is the predicted failure load of the laminate. For the Tsai-Hill and the Tsai-Wu criteria, the predicted laminate failure loads are 5798 lb and 5275 lb, respectively.

C. Failure Predictions Based on Three-Dimensional Stresses

A procedure similar to that just described for CLT stresses is used to predict failure based on finite-element results. Because the region of interest in the free-edge problem is subjected to a three-dimensional state of stress, a three-dimensional failure criterion must be used. The three-dimensional form of the Hoffman criterion is used because its provision for different strengths in tension and compression is an improvement over the Tsai-Hill criterion, and the interaction term of the Tsai-Wu criterion need not be evaluated. If for a lamina $Y_t = Z_t$, $Y_c = Z_c$, and $S_{xz} = S_{xy}$, then the three-dimensional form of the Hoffman failure criterion is

$$\begin{aligned} & \left(\frac{1}{Y_t Y_c} - \frac{1}{2X_t X_c}\right)(\sigma_y - \sigma_z)^2 + \frac{1}{2X_t X_c}(\sigma_z - \sigma_x)^2 \\ & + \frac{1}{2X_t X_c}(\sigma_x - \sigma_y)^2 + \left(\frac{1}{X_t} - \frac{1}{X_c}\right)\sigma_x + \left(\frac{1}{Y_t} - \frac{1}{Y_c}\right)\sigma_y \\ & + \left(\frac{1}{Y_t} - \frac{1}{Y_c}\right)\sigma_z + \frac{1}{S_{yz}^2}\tau_{yz}^2 + \frac{1}{S_{xz}^2}\tau_{xz}^2 + \frac{1}{S_{xy}^2}\tau_{xy}^2 = 1 \quad (4) \end{aligned}$$

Stresses that are rapidly increasing near the free edge cannot be used to calculate the laminate failure load because of the mathematical singularity that presumably exists at the free edge. This restriction prevents calculation of a failure load based on finite-element results for the unreinforced NASA edge delamination tension specimen. For the capped specimen, however,

the ultimate load prediction is based on stresses calculated for a point away from the free edge. At this point, σ_z reaches a maximum value. Following is the failure sequence for the capped specimen as predicted with finite-element results and the three-dimensional Hoffman failure criterion:

1) The 90-deg layers fail in the x -direction (i.e., transverse to the fibers in Fig. 2) as in the two-dimensional stress case. The properties E_x , ν_{xy} , ν_{xz} , G_{xy} , and G_{xz} are then reduced in the finite-element model.

2) The 90-deg layers fail in the z -direction (delamination in Fig. 2). To simulate this failure mode, E_z , ν_{zy} , ν_{zx} , and G_{yz} are reduced in the row of elements closest to the midplane. Another iteration results in the second row of elements having its properties degraded as in step 1. In both cases, the material properties are degraded only in a region near the edge. The width of this region is equal to the laminate thickness because almost all of the interlaminar stresses occur in this zone.

3) A ± 30 -deg layer unit fails due to fiber tension, in-plane shear, z -direction tension, and interlaminar shear. Thus, the laminate fails because no load-carrying fibers remain.

The calculated failure load is 3920 lb. However, this failure prediction is based on several assumptions and approximations, especially concerning simulation of delaminations in step 2. The simulation of x -direction failure in the 90-deg layers, step 1, is relatively straightforward in that when some of the matrix material fails, the rest of the material is strained more. Therefore, all of the matrix material is reasonably expected to fail at approximately the same load. This situation is not true for delamination because a through-the-thickness failure in some of the laminate reduces the stresses in the remaining laminate. Thus, the nature of the simulation of the delamination process has a strong effect on the calculated failure load. Therefore, this failure load is calculated only for comparison purposes and cannot be construed as a failure prediction with a high degree of confidence. However, the events in the predicted progressive failure model are essentially consistent with the actual degradation observed by O'Brien.⁸ The model for the first two steps in the present progressive failure process is depicted in Fig. 2 in which the various degradation zones are shown.

The failure load predicted using finite-element results is 74% of the failure load predicted using CLT. Thus, interlaminar normal stresses make a large contribution to the failure of the laminate, even for the capped laminate with interlaminar normal stresses that are much lower than those for the uncapped laminate.

Similar failure analyses can be performed to evaluate further the alternative edge-cap designs studied by Howard, Gossard, and Jones¹ (see Fig. 18 and Table 3 in Part I). The predicted failure loads based on three-dimensional stresses are 3710 lb for a laminate reinforced with the ± 45 -deg Kevlar-epoxy cap and 3980 lb for a laminate reinforced with the graphite-epoxy cap. These results are obtained with finite-element models that include a gap between the cap and the laminate edge, whereas the results in Table 3¹ are for "ideal" caps. The ± 45 -deg Kevlar-epoxy cap is shown to be the best design for reducing stresses in the ± 30 -deg layers, whereas the graphite-epoxy cap is shown to be the best choice when a gap is present and a progressive laminate failure analysis is used. Therefore, when a gap is present, stiffening of the cap in the z -direction appears to be the best edge-cap design philosophy.

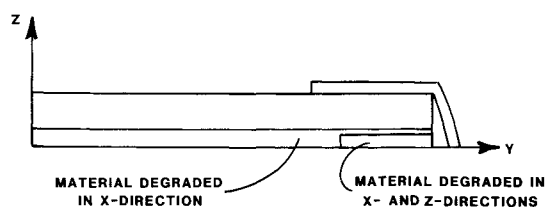


Fig. 2 Model for progressive laminate degradation.

Table 2 Fatigue loading results

	Maximum load, lb	Cycles to failure
Uncapped	1400	100,000 ^a
	1400	6,650
	1300	4,530
Capped	3500	2,580
	3300	2,920
	3300	4,810
	3100	12,290
	3000	11,460

^aSpecimen did not fail.

Table 3 Summary of actual and predicted static tension failure loads

		Failure load, lb	Two-dimensional Hoffman criterion failure load, %
Predicted	Hoffman criterion	5294	100
	Two-dimensional Tsai-Hill criterion	5798	109.5
	Two-dimensional Tsai-Wu criterion	5275	99.6
	Three-dimensional Hoffman criterion	3920	74.1
Actual	Uncapped specimens	1808	34.2
	Capped specimens	4367	82.5

Finite-element analysis is used to show that the interlaminar normal stresses are lower for capped laminates than for uncapped laminates.¹ This result leads to the qualitative conclusion that the capped laminate should be stronger than the uncapped laminate. Comparison of failure predictions based on CLT and finite-element results leads to the conclusion that interlaminar normal stresses are large enough to cause a significant decrease in laminate strength, even for the capped laminates. These theoretical conclusions are verified in an experimental program described in the next section.

III. Experimental Verification

Fifteen NASA edge delamination tension specimens were fabricated and loaded to failure. Of these 15 specimens, eight had edge caps. Three of the capped specimens were loaded in static tension, and five were loaded in tension-tension fatigue. Of the seven remaining uncapped specimens, four were loaded in static tension, and three were loaded in fatigue. For both the static and fatigue loadings, the capped specimens were significantly stronger than the uncapped specimens. The addition of edge caps to the static-test specimens also significantly decreased the coefficient of variation of the failure strength.

A. Fabrication of Specimens

The specimens were cut from cured 12-in. \times 12-in. flat laminates. The laminates were laid up from unidirectional composite material composed of T-300 graphite fibers in a 5209 epoxy resin matrix and cut from the same 12-in.-wide roll of material.

After the laminates were laid up, they were placed in a curing assembly consisting of scrim cloth, bleeder cloth, mylar sheets, and steel plates. The glass scrim cloth prevents the bleeder cloth from sticking to the graphite-epoxy laminate, the bleeder cloth absorbs excess resin during cure, and the mylar sheets

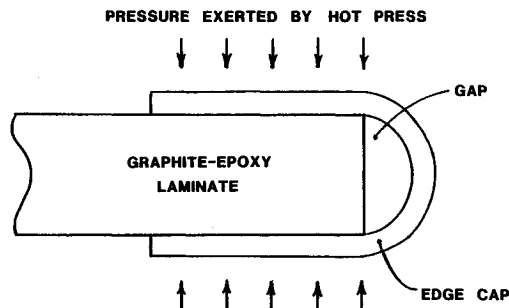


Fig. 3 Gap that developed during curing.

prevent the bleeder cloth from sticking to the steel plates. The curing assembly was placed in a hot press that had been heated to 170°F. A small force was applied on the press to ensure contact between the components of the curing assembly. The initial temperature was held at 170°F for 30 min to allow the temperature to equilibrate. The force on the press was then increased until the laminate was subjected to 100 psi pressure. Next, the temperature was increased to 260°F for 1 h and 35 min whereupon the heaters were turned off. The pressure was held at 100 psi until the temperature dropped to 180°F. Then, the press was opened, the curing assembly was removed from the press, and the laminate was separated from the rest of the curing assembly.

The cured laminates were cut into 1.5-in.-wide by 10-in.-long specimens with a diamond-tipped saw. One-in.-wide Kevlar reinforcements were cut from a sheet of style-120 Kevlar-49 cloth preimpregnated with F-155 epoxy resin and placed over the free edges of the laminates. These capped laminates were then subjected to a cure cycle similar to the earlier cure cycle, i.e., the caps were fastened to the laminate by a secondary bonding operation.

During edge-cap curing, no pressure was exerted to hold the cap against the laminate edge. As a result, a gap between the laminate edge and the cap existed in all of the reinforced specimens, although the gap was not as regular as depicted in Fig. 3. For laminates thicker than the NASA edge delamination tension specimen, this gap could be prevented by using a curing apparatus through which pressure is applied to the laminate edges or by which the cap is restrained from moving away from the edge as in Fig. 4. For the thin laminates used in this project, such an apparatus would probably not prevent the gap because the Kevlar fibers could not be bent at a sufficiently small radius. No excess resin was evident in the gap, and so the gap was modeled as a void area in the finite-element analysis of the reinforced specimens with gaps present (see Sec. II.D of Ref. 1).

B. Test Apparatus and Procedures

Static and constant-amplitude tension-tension fatigue tests were performed in a 20,000-lb-capacity MTS servohydraulic tension-compression-fatigue machine operated in the load-control mode. Each specimen was placed in 2-in.-wide grips so that both ends were clamped across the full specimen width. The loading rate for static tension tests was 25 lb/s. The specimen load was monitored by a digital voltage readout from the function generator as well as an *x-y* plotter with input from the load cell. No strains were measured. Tension-tension fatigue tests were performed as follows:

- 1) Specimens were loaded to the average of the high and low loads. The low load was always 100 lb to ensure that load variations did not cause compression of the specimen. The high load was selected to obtain a variety of stress levels for the load vs number of cycles curve.
- 2) The load-function generator was set to generate a sine wave at a loading frequency of 10 cycles/s with initial zero amplitude.
- 3) The sine-wave loading was begun, and the amplitude of the sine wave was slowly increased until the desired loading

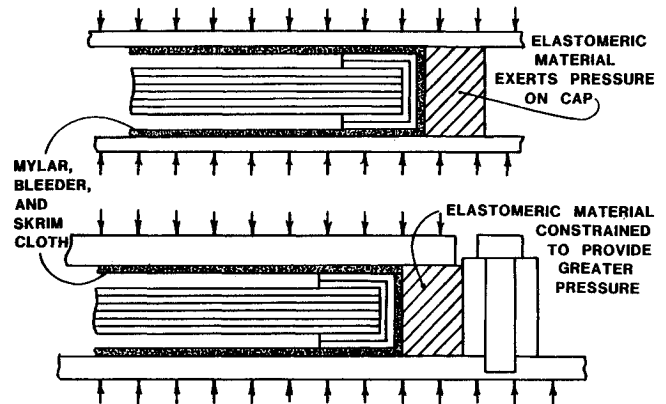


Fig. 4 Curing assemblies that prevent a gap.

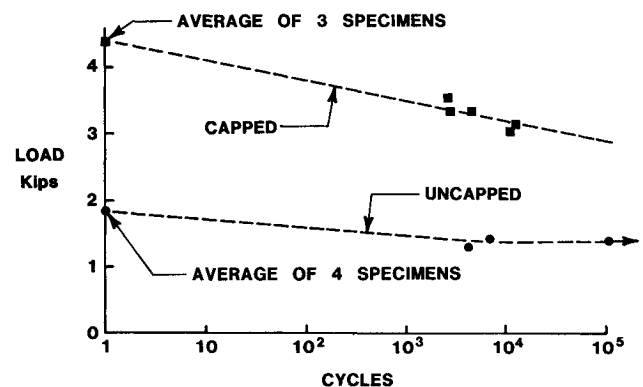


Fig. 5 Load vs number of cycles curve of experimental results.

level had been reached. The number of cycles to reach this loading was recorded and later subtracted from the number of cycles to reach failure. Normally, 200–300 cycles were required to reach the desired loading.

- 4) The specimen was loaded until failure occurred, and the number of cycles to failure was recorded.

C. Test Results

The average static tension failure load of the four uncapped specimens was 1808 lb. The failure loads of the specimens varied widely over a range of 1380–2250 lb, with a coefficient of variation of 24%. The three capped specimens failed at an average load of 4367 lb. The highest failure load obtained was 4650 lb, the lowest was 3950 lb, and the coefficient of variation was only 8%. Specific static test results are listed in Table 1.

Results for the three uncapped and five capped specimens that were loaded in tension-tension fatigue are shown in Table 2. The results, along with those for the static tension tests, are plotted on a load vs number of cycles to failure curve in Fig. 5. The lines of the fatigue curve are straight-line, least-squares fits of the data points. The results corresponding to 10,000 load cycles—1400 lb for the uncapped specimens, and 3160 lb for the capped specimens—are obtained from the least-squares fits of the data points. The strength increase from the unreinforced to the reinforced specimens is almost the same for 10,000 cycles (about 130%) as for the static tests (about 140%).

Different failure modes occurred for uncapped vs capped specimens. The failed uncapped laminates have delamination along the free edges and fail along directions parallel to the fibers as seen in the photograph of a typical failed uncapped laminate in Fig. 6. No fiber breakage is evident in the uncapped specimens. In contrast, the failed capped laminates have broken graphite fibers in the ± 30 -deg layers as seen in Fig. 7.

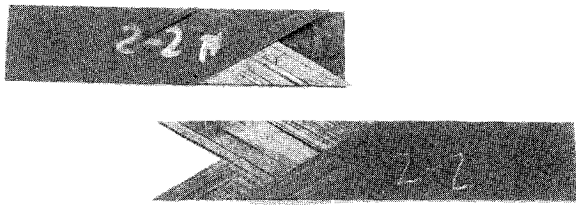


Fig. 6 Failed uncapped specimens.

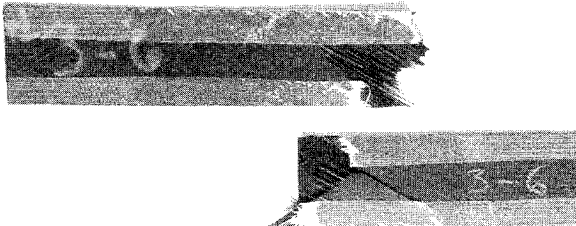


Fig. 7 Failed capped specimens.

The results of the experimental portion of this project demonstrate that adding edge caps increases laminate strength and lowers the coefficient of variation of the strength, hence increases the structural reliability. These experimental results are correlated with the theoretical results in the next section.

D. Theoretical-Experimental Results Correlation

SAAS III finite-element analyses were used by Howard, Gossard, and Jones¹ to show that adding edge caps to the NASA edge delamination tension specimen causes a significant reduction in σ_z . Thus, capped specimens should achieve a higher failure load than uncapped specimens. A finite-element model with a gap between the cap and the edge of the specimen is used to show that σ_z can be reduced, even by adding imperfect edge caps to the specimens. The experimental results are in agreement with these qualitative theoretical results. The capped specimens, all of which had gaps between the caps and the specimen edges, failed at an average static tension load of 4367 lb, whereas the uncapped specimens failed at an average load of 1808 lb.

The Hoffman failure criterion was used to relate failure of the specimens to calculated interlaminar stresses. The two-dimensional form of the criterion was used to predict failure of the specimen in a region where no interlaminar stresses exist. Then, the three-dimensional form of the criterion was used to predict failure of the capped specimen by taking into account actual cap geometry in a finite-element analysis. The same procedure could not be used for the uncapped laminate because stresses calculated for the region adjacent to the free edge must be used in the failure prediction. These stresses are increasing very rapidly near the edge, an indication of a possible mathematical singularity. Because such singularity is simply a manifestation of the necessarily approximate linear mathematical model and not representative of physical reality, the stresses calculated for this region cannot be considered accurate.

For the capped specimens, the predicted failure load calculated using the three-dimensional failure criterion is 74% of the load calculated using the two-dimensional failure criterion. In the static load tests, the capped specimens failed at an average of 82% of the two-dimensional failure prediction. Therefore, the analysis is used to show the relative impact of the interlaminar stresses, but cannot be used to accurately predict the failure load (the predicted failure load is 10% different from the actual failure load). The predicted and measured failure loads are summarized in Table 3.

Several reasons are possible for the difference between predicted and actual failure loads. One is that the material strengths might be somewhat different from those used in the

calculations. In addition to the uncertainty of the strength values, the material was stored about 10 years beyond its expiration data. The actual specimen strength, however, was higher than the predicted strength, so degradation of the material apparently was not a factor. The most likely reason for the difference between theoretical and experimental results is the difficulty in simulating delaminations in the analysis. A good method for accounting for delaminations in finite-element analysis must be developed before accurate failure predictions can be made for laminates in which interlaminar stresses are significant.

IV. Concluding Remarks

The conclusions drawn from this study are summarized. Next, possible applications of the reinforcing concept are given. Finally, problems are identified for examination in future research efforts.

A. Conclusions

The conclusions drawn from the theoretical and experimental results of this project are as follows:

- 1) Effective U-shaped edge caps for thin laminates can be fabricated easily without special tooling or complex procedures.
- 2) Laminates that tend to delaminate have higher strength when edge caps are applied than laminates without reinforcement. The strength increase measured for the statically loaded specimens is about 140%. A similar increase (130%) occurs for fatigue-loaded specimens at a specific life (10,000 cycles). Thus, to carry a prescribed load or to last a prescribed life, an uncapped laminate must be more than twice as thick as a laminate with edge caps. Moreover, the coefficient of variation of static tensile strength is reduced from 24% to 8% by capping the edges (based on a limited statistical sample but with normal engineering significance). This reduction in coefficient of variation permits the allowable load of the structure to be increased because the structure has been made much more reliable. Accordingly, edge caps lead to substantial weight savings and increases in structural reliability.
- 3) The load carried in the cap is inherently included in the capped specimen failure loads. The influence of a single layer as one layer of an 11-layer laminate is quite small (9%), but the effect of the cap is to increase the failure load by 130–140%. Thus, the real influence of the cap is the restraint of free-edge delamination, i.e., the fundamental failure mode changes. Accordingly, the addition of a cap is quite unlike the addition of merely another layer of material to a laminate.
- 4) Finite-element analysis is used in Part I¹ of this paper to qualitatively show reinforcement effectiveness and to evaluate different edge-cap designs. Cap-to-laminate bond length and cap thickness are shown to have little influence on cap effectiveness, but cap material and fiber orientation strongly affect cap performance.
- 5) The predicted failure load for the reinforced laminate based on finite-element results and a progressive laminate failure analysis using the Hoffman three-dimensional failure criterion is 10% lower than the actual failure load. The major problem in predicting this load is uncertainty in simulating delaminations.

The NASA edge delamination laminate was selected for this study because of a strong tendency to delaminate. Thus, the very large increases in strength shown here should not be expected for general laminates. However, the edge-reinforcement concept can be applied to practical structures with free edges with significant benefits. Some possible applications are suggested in the next section.

B. Possible Applications

The edge-reinforcement concept can be applied to many structures that contain free edges as shown in the following examples. Composite panels are often reinforced with laminated stiffeners that have free edges. Edge caps could be added

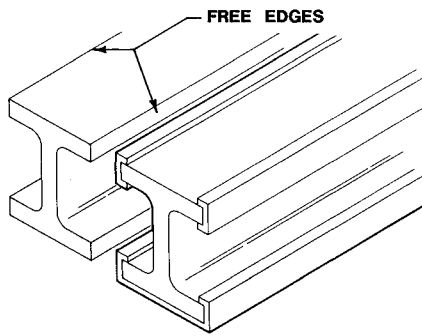


Fig. 8 Reinforcement of a laminated stiffener.

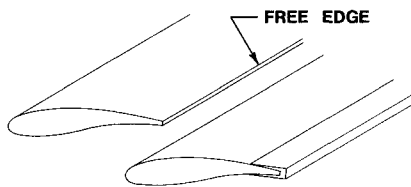


Fig. 9 Reinforcement of the trailing edge of an aileron.

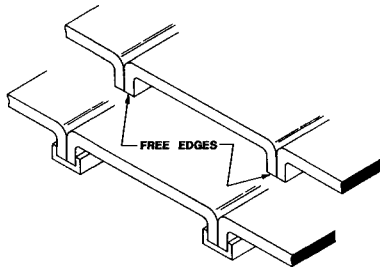


Fig. 10 Reinforcement of aircraft fuselage panels.

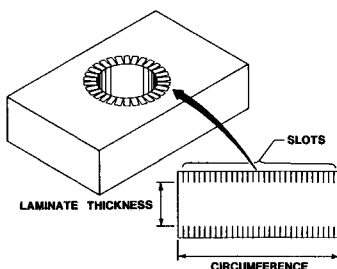


Fig. 11 Reinforcement of a hole.

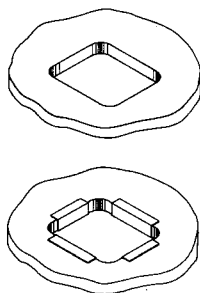


Fig. 12 Reinforcement of a cutout.

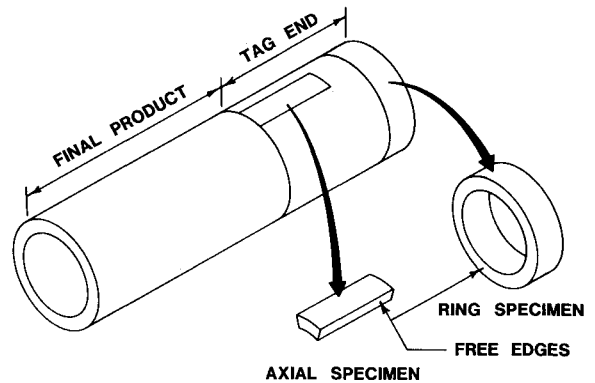


Fig. 13 Reinforcement of tag-end test specimens.

Although curved edges are more difficult to reinforce than straight edges, circular holes can be reinforced. First, a slightly oversized hole is drilled through the laminate. The reinforcements are rectangular pieces of material (usually woven for ease in handling) with a length equal to the circumference of the hole. The reinforcement is cut or slotted perpendicular to the edges so that small areas of the material can be folded over and bonded to the top and the bottom of the laminate as shown in Fig. 11. The slots must be closely spaced so that the reinforcing material will readily conform to the hole shape. To obtain the proper hole diameter, an expanding device or a fixed-diameter plug would then be placed in the hole and would remain during the curing process. Although several problems might arise from this method of reinforcement (clearance problems at the top and the bottom of the laminate, quality assurance problems, etc.), it has the potential of strengthening a laminate with holes. Preliminary favorable results are a demonstration of manufacturing feasibility and design effectiveness. Moreover, O'Brien and Raju⁹ have shown that mode I delamination dominates around open holes, so this reinforcement concept should be successful.

Cutouts in laminates could easily be reinforced with edge caps. Cutouts are usually not load-bearing holes, and so their shapes are not dictated by fastener shapes. Therefore, rectangular cutouts (with rounded corners) are not uncommon and could be reinforced easily. An edge cap could be used along each side of the rectangle and around each corner as shown in Fig. 12. An example of a possible use of this concept is a rocket motor skirt, which is a cylindrical or conical structure attached to one end of a rocket motor. The skirt must be capable of reacting a compressive load equal to the rocket motor thrust. Wiring, hydraulic lines, etc., pass through cutouts in the skirt to the rocket ignitor or the nozzle actuation system. Reinforcing the free edges of these cutouts could strengthen the skirt and thus allow a thinner, lighter skirt.

Another good candidate for free-edge reinforcement is the so-called tag-end test specimen that is used to determine the strength of a filament-wound cylindrical shell. Filament-wound shells are usually fabricated longer than the final product, and the length of shell that is cut off is called the tag end as in Fig. 13. Test specimens used to characterize the shell material are cut from the tag end. These specimens are accurate representations of the final product because they were made with the same manufacturing processes. The test specimens, however, have free edges, unlike the final product. Reinforcing the free edges would prevent edge stresses from causing the specimens to have a drastically lower strength than the final product. Therefore, a more representative strength evaluation of the shell could be performed.

Actually, the logical extension of the preceding argument affects all laminate strength evaluations. Edge-cap reinforcements more nearly enable measurement of the true strength of a laminate by eliminating the free edges that cause an unrealistic strength degradation in test specimens. Accordingly, all small laminate test specimens should have edge caps.

to these stiffeners as shown in Fig. 8. The cap on the bottom extends across the full width of the stiffener so that the stiffener can be placed flat against the panel. Composite ailerons are being used increasingly in the aerospace industry, and the trailing edge of an aileron is a free edge, which could be capped as shown in Fig. 9. Aircraft fuselage panels could be joined with edge caps as shown in Fig. 10. In all these applications, the edge cap also serves as a moisture barrier.

Many possible applications of the free-edge reinforcement concept exist, and more will arise as laminated composite materials usage expands. Before these applications can be developed, more research, both theoretical and experimental, must be performed so that problems and potentials associated with the reinforcements are better understood.

C. Suggestions for Future Work

Future research work concerning the free-edge reinforcement concept is suggested in this section. These suggestions are classified as either theoretical or experimental, although any further research should combine elements of both. That is, any theoretical studies should be experimentally verified, and any experimental studies should be extended by suitable theoretical work in order to attain results of design significance.

1. Theoretical Work

As Pagano and Pipes¹⁰ note, attempts to refine approximate solutions for the free-edge problem are probably of little value. However, development of better techniques for simulating delaminations would be beneficial. Failure of a laminate depends on redistribution of interlaminar stresses within the laminate. Therefore, the manner in which delaminations are modeled strongly influences the predicted failure load.

Analysis of more complex structures, such as a reinforced hole in a laminate, could show whether additional work is warranted. As in this paper, an exact or highly accurate approximate solution is not needed to show the effects of adding reinforcement. Reinforcement concepts that appear to be effective could then be studied in an experimental program.

2. Experimental Work

Only the NASA edge delamination tension specimen is addressed in this paper, and the experimental portion of the project is restricted to only one edge-cap design. A logical follow-up to this work would be a more comprehensive experimental program dealing with different laminates and cap designs. In particular, thick laminates should be studied because they can be reinforced more easily than thin laminates. Caps could be of different materials, different fiber orientations, and different physical dimensions (thickness, bond length, etc.). Also, different manufacturing methods should be compared. For thick laminates, the concept of placing an already cured edge cap on a laminate should be compared with the concept of curing the cap in place.

In addition to further work with flat laminate free edges, more complicated reinforcement applications should be studied experimentally. Among these applications, cutouts and loaded holes in laminates under both tensile and compressive loads appear to have significant potential.

Additional research on edge reinforcements should incorporate, to some degree, both theoretical and experimental work. Although conclusions about a reinforcement's ability to increase laminate strength can be reached using only experimental results, an opportunity exists to use analysis to better understand the nature of interlaminar stresses near the edges. On the other hand, because of the approximate nature of the analysis, the actual strength increase brought about by the addition of reinforcement can only be determined experimentally.

Free-edge reinforcements can have a positive influence on laminate strength in many situations. The next step is to apply the reinforcement concept to actual structures.

Acknowledgments

This work was sponsored by NASA Langley Research Center under Grant NAG-1-389. Interaction with the monitor, Mark J. Shuart, is appreciated.

References

- ¹Howard, W. E., Gossard, T., Jr., and Jones, R. M., "Composite Laminate Free-Edge Reinforcement with U-Shaped Caps, Part I: Stress Analysis," *AIAA Journal*, Vol. 27, May 1989, pp. 610-616.
- ²O'Brien, T. K., "Mixed-Mode Strain-Energy-Release Rate Effects on Edge Delamination of Composites," *Effects of Defects in Composite Materials*, American Society for Testing and Materials, Philadelphia, PA, ASTM STP 836, 1984, pp. 124-142.
- ³"ST-2: Specification for Edge Delamination Tension Test," NASA Reference Publication 1092, July 1983, pp. 7-14.
- ⁴Azzi, V. D. and Tsai, S. W., "Anisotropic Strength of Composites," *Experimental Mechanics*, Sept. 1965, pp. 283-288.
- ⁵Hoffman, O., "The Brittle Strength of Orthotropic Materials," *Journal of Composite Materials*, April 1967, pp. 200-206.
- ⁶Tsai, S. W. and Wu, E. M., "A General Theory of Strength for Anisotropic Materials," *Journal of Composite Materials*, Jan. 1971, pp. 58-80.
- ⁷Narayanaswami, R. and Adelman, H. M., "Evaluation of the Tensor Polynomial and Hoffman Strength Theories for Composite Materials," *Journal of Composite Materials*, Oct. 1977, pp. 366-377.
- ⁸O'Brien, T. K., "Characterization of Delamination Onset and Growth in a Composite Laminate," *Damage in Composite Laminates*, edited by K. L. Reifsnider, American Society for Testing and Materials, Philadelphia, PA, ASTM STP 775, 1982, pp. 140-167.
- ⁹O'Brien, T. K. and Raju, I. S., "Strain-Energy-Release Rate Analysis of Delamination Around an Open Hole in Composite Laminates," *Proceedings of the 25th AIAA/ASME/ASCE/AME Structures, Structural Dynamics, and Materials Conference*, AIAA, New York, May 1984, pp. 526-536.
- ¹⁰Pagano, N. J. and Pipes, R. B., "Some Observations on the Interlaminar Strength of Composite Laminates," *International Journal of Mechanical Sciences*, Aug. 1973, pp. 679-688.